Journal of Materials Science: Materials in Electronics (2018) 29:8964–8969
https://doi.org/10.1007/s10854-018-8918-2

Scintillation and dosimeter properties of ^{6}LiF/CaF$_2$:Eu eutectic composites

Naoki Kawano[1] · Noriaki Kawaguchi[2] · Kentaro Fukuda[3] · Go Okada[2] · Takayuki Yanagida[2]

Received: 15 February 2018 / Accepted: 14 March 2018 / Published online: 22 March 2018

Abstract

We investigated scintillation and dosimeter properties of ^{6}LiF/CaF$_2$ eutectic composites doped with different concentrations of Eu (0.005, 0.02, 0.1, 0.3, and 1.0). In the photoluminescence (PL) and scintillation spectra, an emission peak at 430 nm due to the 5d–4f transitions of Eu^{2+} was observed. The intensity of PL and scintillation for ^{6}LiF/CaF$_2$:0.005%Eu was the highest among the samples tested. In thermally stimulated luminescence (TSL), several glow peaks of ^{6}LiF/CaF$_2$:0.005%Eu were observed after X-ray irradiation of 1000 mGy. The TSL response exhibited a linear response against X-ray dose over a dose range of 1–10,000 mGy. In optically stimulated luminescence (OSL), an emission peak was observed at 430 nm during a stimulation by 630 nm light after X-ray irradiation of 1000 mGy. The OSL intensity was the highest for ^{6}LiF/CaF$_2$:0.005%Eu among all the samples investigated.

1 Introduction

Radiation dosimetric methods have attracted much attention for decades in order to measure radiation dose [1–4]. They generally utilize phosphor materials, which show radiation-induced luminescence phenomena: thermally-stimulated luminescence (TSL), optically-stimulated luminescence (OSL), and radio-photoluminescence (RPL). In TSL and OSL, electrons and holes generated by ionizing radiations are trapped at localized centers; and these charges are de-trapped by external stimulation and recombine at luminescence centers. The luminescence stimulated by thermal energy is called TSL whereas the one stimulated by light is called OSL. In contrast, RPL is a phenomenon that a new luminescence center is formed by ionizing irradiations; therefore, the photoluminescence (PL) intensity of the newly created emission center is proportional to the irradiation dose. In these dosimetric methods, knowing a relationship between dose and emission intensity, namely a dose response function, allows us to determine the irradiated dose. The TSL dosimetry technique has been established in the past decades and has found many useful applications in various fields. There are many commercial TSL dosimeter systems, which are especially utilized for individual radiation monitoring applications. In such applications, the effective atomic number of dosimeter materials is preferred to be close to that of biological tissue ($Z_{eff} = 7.35$–7.65) [5] because interaction probability and mechanism of ionizing radiations with matter strongly depend on the chemical composition of materials. In the past studies, many kinds of TSL materials such as LiF, CaF$_2$, CaSO$_4$, MgB$_4$O$_7$ have been developed [1].

Among the TSL materials, LiF is one of the most widely used compounds. Many researchers investigated the TSL properties of LiF undoped and doped with impurities. LiF:Mg,Ti has been known as TLD-100 and is a commercial product. It exhibits a TSL glow peak around 200 °C, and the TSL response is linear against irradiation dose with the dynamic range of 20 μGy–10 Gy [1]. Besides, it has been reported that LiF:Mg,Cu,P is more sensitive than that of LiF:Mg,Ti [6, 7]. Moreover, ^{6}LiF:Mg,Cu,P has been investigated for neutron dosimetry because ^{6}Li has a high interaction probability with thermal neutrons due to the nuclear reaction of ^{6}Li (n, α)^{3}H with high Q-value of 4.8 MeV [8–16]. In addition to LiF, CaF$_2$ is well-known to show notable TSL properties. In fact, CaF$_2$:Mn is equipped

✉ Naoki Kawano
n-kawano@gipc.akita-u.ac.jp

1 Graduate School of Engineering Science, Akita University, 1-1 Tegata Gakuen-machi, Akita 010-8502, Japan

2 Graduate School of Materials Science, Nara Institute of Science and Technology, 8916-5 Takayama, Ikoma, Nara 630-0192, Japan

3 Tokuyama Corporation, 1-1, Mikage-cyo, Shunan-shi, Yamaguchi 745-8648, Japan

in another commercial dosimeter (TLD-400), and it shows a glow peak at 260 °C with a linear dose response function over 0.5 mGy—a few kGy [17]. In addition to CaF_2:Mn, TSL dosimeter properties of CaF_2:Dy and CaF_2:Tm have been investigated [18].

Although TSL properties of each LiF and CaF_2 have been intensively investigated individually for decades, very few studies reported the dosimeter properties of LiF/CaF_2 eutectics compounds. This eutectic system of LiF/CaF_2 can be formed at the eutectic composition (LiF:CaF_2 = 80:20 mol%) [19–23]. In general, eutectic compounds have excellent bonding between different phases with better mechanical properties and thermal shock resistance than those of single crystals and conventional ceramics [20]. Moreover, the effective atomic number of LiF/CaF_2 eutectic compound (Z_{eff} = 9.86) is close to that of the soft tissue of human body (Z_{eff} = 7.35–7.65) [5]. Therefore, LiF/CaF_2 eutectic compounds are a promising candidate for individual dosimetry applications. In the past research, LiF/CaF_2:Mn eutectic composite was first proposed for dosimeter applications [19]. The paper reported TSL peaks at 130 °C associated with the LiF phase and at 275 °C with the CaF_2 phase were observed after X-ray irradiation [19].

In this study, we fabricated ^{6}LiF/CaF_2 eutectic compounds with different concentrations of Eu. It has been reported that dosimeter properties of each LiF and CaF_2 were enhanced by an incorporation of Eu in the past studies [24, 25]. Moreover, ^{6}LiF/CaF_2 eutectic compounds are potential materials as neutron dosimeters because the eutectic materials contain ^{6}Li, and it has a considerably low sensitivity to background γ-rays due to the low density [8–16]. In this work, we investigated PL and scintillation properties of ^{6}LiF/CaF_2 eutectic compounds with different concentrations of Eu. Following these characterizations, the storage luminescence properties such as TSL and OSL were also evaluated for dosimeter applications.

2 Experimental

High purity (99.99%) fluoride powders of ^{6}LiF (95% enriched), CaF_2 and EuF_3 were used as the starting materials. The ^{6}LiF and CaF_2 were mixed at 80:20 molar ratio, which corresponds to the eutectic composition, and a fraction of EuF_3 was added (0.005, 0.02, 0.1, 0.3, and 1.0% with respect to that of CaF_2). These materials were loaded into a graphite crucible, and the micro-Bridgman method was used to produce ^{6}LiF/CaF_2:Eu [21, 26]. The crucible was placed and surrounded by carbon resist heaters inside a stainless chamber. The crucible was heated up to 400 °C and kept for about 8 h in vacuum (10^{-4} Torr). After the baking, the chamber was filled with high purity Ar (99.999%) and CF_4 (99.999%) gases until ambient pressure. The ratio of Ar and CF_4 was 9:1. Further, the crucible was heated up to 800 °C and then kept for 30 min. Finally, the heater was stopped and cooled to room temperature with a cooling rate of 5 °C/min. After the fabrication process, the samples were cut and polished into pieces of size of $1 \times 2 \times 5$ mm^3 to investigate scintillation and dosimeter properties. As shown in Ref. [21] and Ref. [26], Eu-doped samples had ordered lamellar structures [21, 26].

Quantum yield (*QY*) values and PL excitation/emission contour graphs were evaluated by using Quantaurus-QY (Hamamatsu Photonics). PL decay time profiles were evaluated by using Quantaurus-τ (Hamamatsu Photonics). In these measurement, the excitation wavelength was 340 nm, and the monitoring wavelength was 430 nm. X-ray induced scintillation spectra were measured using our lab-constructed setup [27]. The samples were excited using an X-ray generator in which the applied tube voltage and current were 40 kV and 1.2 mA. The mean energy of the X-ray was approximately 26 keV. The scintillation was guided to Ocean Optics CCD-based spectrometer (QEPro). Further, the scintillation decay time profile was measured using an afterglow characterization system equipped with a pulse X-ray tube [28]. The applied voltage to the pulse X-ray source was 30 kV. TSL glow curve was measured using a Nanogray TL-2000 after X-ray irradiation [29]. The heating rate used for all the TSL measurements was fixed to 1 °C/s, and the samples were heated from 50 to 490 °C to measure. The dose used was the value in air at the sample entrance. Further, OSL spectrum was measured under 630 nm stimulation by using Quantaurus-τ (Hamamatsu Photonics).

3 Results and discussion

Figure 1 represents PL and excitation contour graphs of ^{6}LiF/CaF_2:Eu. The ^{6}LiF/CaF_2:0.005–1.0%Eu exhibited an emission at 430 nm under the excitation wavelengths across 320–410 nm. The emission wavelength of ^{6}LiF/CaF_2:Eu agreed well with that of CaF_2:Eu reported in the past study [30]. Therefore, this emission could be attributed to the 5d–4f transitions of Eu^{2+} [26, 30]. In addition, *QY* values of ^{6}LiF/CaF_2:Eu are also shown in Fig. 1. The *QY* values were 0.76 (Eu:0.005%), 0.54 (Eu:0.02%), 0.49 (Eu:0.1%), 0.19 (Eu:0.3%), and 0.07 (Eu:1.0%). The *QY* value of ^{6}LiF/CaF_2:0.005%Eu was the highest among the present samples tested. The *QY* value decreased with increasing the concentration of Eu. The reason was blamed for concentration quenching.

Figure 2 exhibits PL decay time profiles of ^{6}LiF/CaF_2:Eu. Each decay curve was approximated by exponential functions. The decay time constant of the ^{6}LiF/CaF_2:0.005%Eu sample (λ_{em} = 430 nm, λ_{ex} = 340 nm) was 705 ns. The decay time was almost the same as the typical time constant for

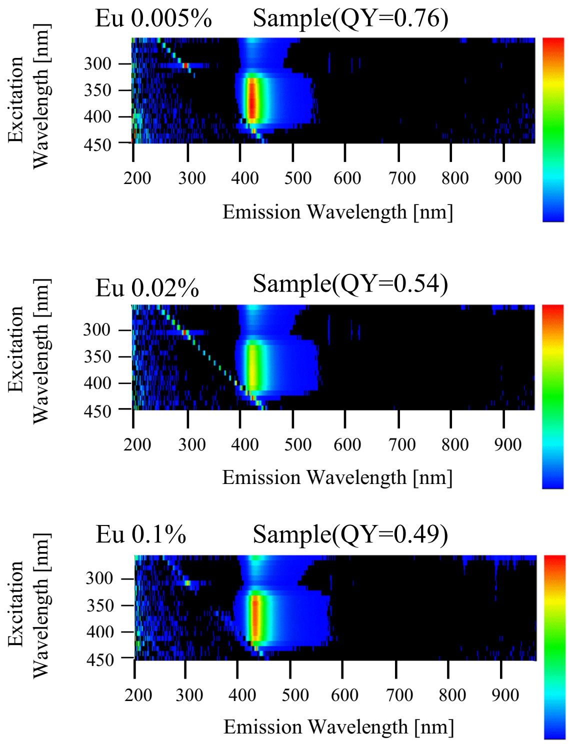

Fig. 1 PL and excitation contour graphs of ^{6}LiF/CaF_2:Eu

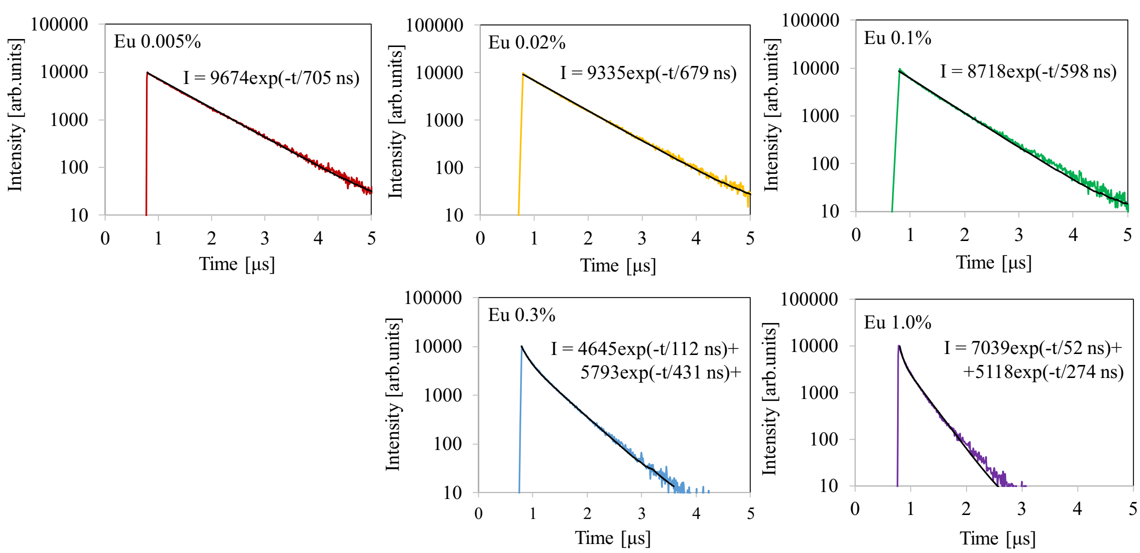

Fig. 2 PL decay time profiles of ^{6}LiF/CaF_2:Eu

the 5d–4f transitions of Eu^{2+} [30–32]. The decay time was faster when Eu concentration was higher due to concentration quenching, suggested by the concentration dependence of PL *QY*.

Figure 3 shows X-ray induced scintillation spectra of ^{6}LiF/CaF_2:Eu. In the spectra, an emission peak was observed around 430 nm. The spectral feature was the same as that in PL; thus, the emission origin was ascribed to the 5d–4f transition of Eu^{2+}. Besides, the scintillation intensity of ^{6}LiF/CaF_2:0.005%Eu sample was the highest among the present samples. The scintillation intensity could be explained by a product of energy migration efficiency and *QY*; thus, the consistency between the PL *QY* and the scintillation intensity could be understood. In addition, a broad emission peak

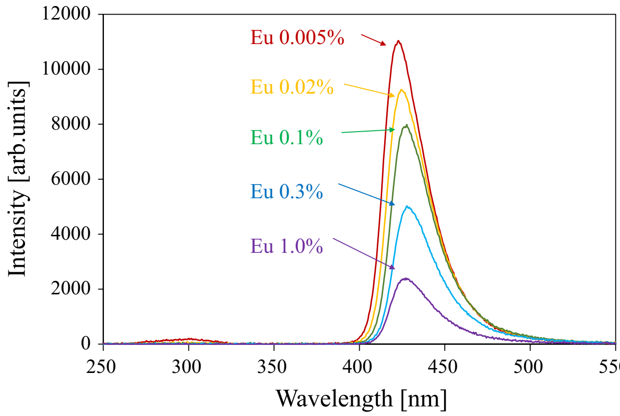

Fig. 3 X-ray irradiated scintillation spectra of $^6LiF/CaF_2$:Eu

at 300 nm was observed in $^6LiF/CaF_2$:0.005%Eu sample. This peak could be ascribed to self-trapped excitons (STE) in ^6LiF and/or CaF_2 host [5, 30, 33].

Figure 4 exhibits X-ray induced scintillation decay time profiles of $^6LiF/CaF_2$:Eu. Each decay curve was approximated by exponential decay functions to derive the decay times. The obtained values for the $^6LiF/CaF_2$:0.005%Eu sample were 225 and 710 ns. The faster component was consistent with the reported value derived by VUV radiation, so the origin of the faster component may be due to STE in CaF_2 host [5, 30, 33, 34]. Further, the slower component was attributed to the 5d–4f transitions of Eu^{2+} as the value was equivalent to that of PL (Fig. 2). The decay time became faster with increasing the concentrations of Eu due to concentration quenching.

Figure 5 shows TSL glow curves of $^6LiF/CaF_2$:Eu. The glow curves were measured after the samples were irradiated by X-rays (1000 mGy). Several glow peaks were observed in the range of 90–280 °C. The TSL intensity of $^6LiF/CaF_2$:0.005%Eu was the highest among the present samples, and it decreased with an increase of Eu concentration. In order to analyze the trap levels, the glow peak temperature and the activation energy were derived by numerical approximations assuming the first-order kinetics. The analysis details can be found elsewhere [35], and Table 1 summarizes the calculation results. The TSL intensity of $^6LiF/CaF_2$:0.3%Eu and 1%Eu was too low to calculate these parameters accurately. The origin of TSL glow peaks around 26–220 °C may be attributed to LiF:Eu and some unknown impurities in the starting materials [19, 24, 30] while the

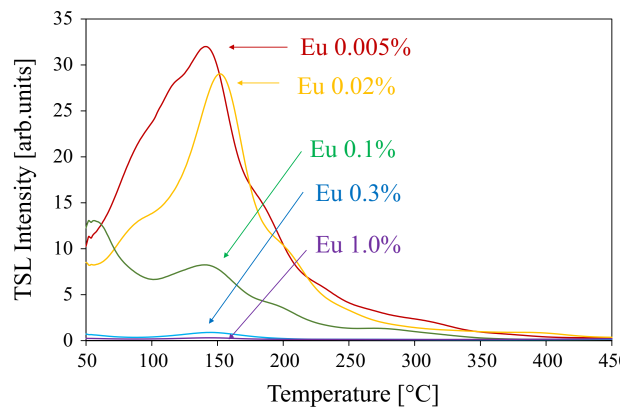

Fig. 5 TSL glow curves of $^6LiF/CaF_2$:Eu

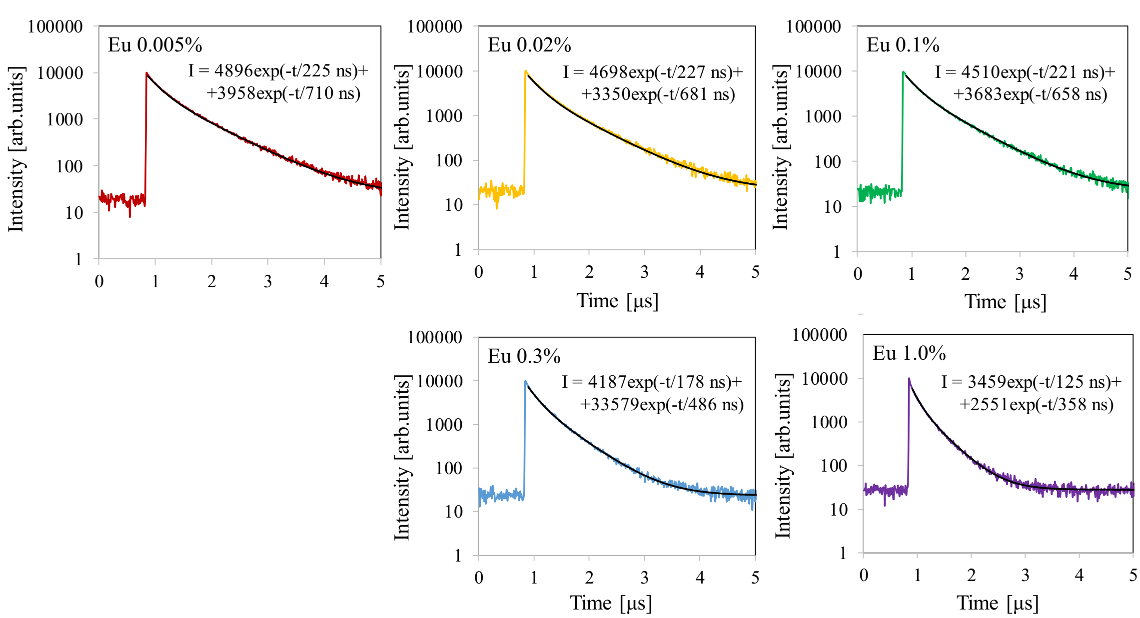

Fig. 4 X-ray irradiated scintillation decay time profiles of $^6LiF/CaF_2$:Eu

Table 1 Maximum peak temperatures and the activation energies of TSL in $^6LiF/CaF_2$:Eu

	Peak 1		Peak 2		Peak 3		Peak 4		Peak 5	
	T_M [°C]	E [eV]	T_M [°C]	E [eV]	T_M [°C]	E [eV]	T_M [°C]	E [eV]	T_M [°C]	E [eV]
Eu0.005%	100	0.4	145	0.7	180	0.7	225	0.8	281	0.9
Eu0.02%	91	0.4	150	0.7	175	0.7	220	0.8	279	0.9
Eu0.1%	92	0.4	141	0.7	174	0.7	221	0.8	282	0.9

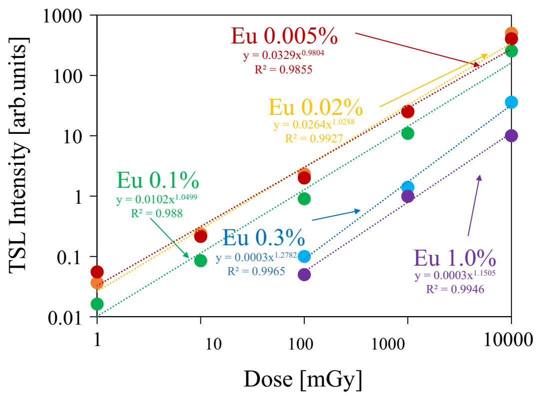

Fig. 6 TSL dose response curves of $^6LiF/CaF_2$:Eu

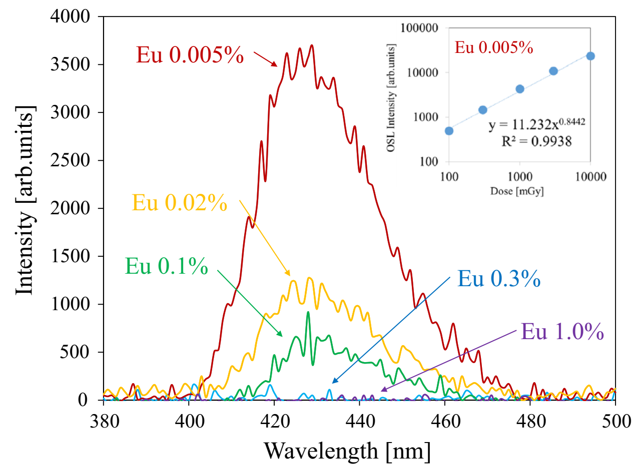

Fig. 7 OSL spectra of $^6LiF/CaF_2$:Eu

origin of TSL glow peak around 280 °C can be associated with CaF_2:Eu [19, 25]. In addition, activation energies and maximum peak temperatures of these TSL peaks were almost the same regardless of the concentrations of Eu. Figure 6 exhibits dose response curves of $^6LiF/CaF_2$:Eu. Here, the glow peak intensity around 140 °C was considered as a signal since it showed a remarkable peak feature. The lower detection limit of $^6LiF/CaF_2$:0.005–0.1%Eu was found to be 1 mGy, and the samples had a linear response against the incident X-ray dose over the dose range of 1–10,000 mGy. Dosimeter having a linear response is advantageous because it enables us to easily and accurately calibrate the dose. As a result, $^6LiF/CaF_2$:0.005–0.1%Eu showed a high TSL dosimeter performance among the present samples since they showed a good dose linearity for low doses.

In order to study deeper traps, we investigated OSL. Figure 7 shows OSL spectra of $^6LiF/CaF_2$:Eu. The samples were irradiated with 1000 mGy X-rays. When the samples were stimulated by 630 nm light, an emission peak was observed at 430 nm, which agreed well with luminescence features of the 5d–4f transitions of Eu^{2+} observed in PL and scintillation. Among the samples tested, the OSL intensity of $^6LiF/CaF_2$:0.005%Eu was the highest, and the intensity of OSL decreased with increasing the concentration of Eu. The dose response curve of OSL for $^6LiF/CaF_2$:0.005%Eu is illustrated in the inset of Fig. 7. The signal was measurable as low as 100 mGy, and the intensity increased monotonically with the irradiation dose. The detected lower limit was much higher than that of commercial OSL materials [1], but the sensitivity can be improved by optimizing the reader setup (the signal was measured by using a conventional spectrofluorometer).

4 Conclusions

We investigated optical, scintillation and dosimeter properties of $^6LiF/CaF_2$:Eu eutectic compounds. The PL *QY* of $^6LiF/CaF_2$:0.005%Eu was the highest among the samples. $^6LiF/CaF_2$:Eu showed PL and scintillation with an emission peak at 430 nm, which was attributed to the 5d–4f transitions of Eu^{2+}. The PL and scintillation decay times of the 5d–4f transitions of Eu^{2+} became faster with increasing the concentration of Eu due to concentration quenching. $^6LiF/CaF_2$:Eu showed TSL with glow curves over 90–280 °C, and $^6LiF/CaF_2$:0.005–0.1%Eu were confirmed to show linear response to the irradiated X-ray dose over a range of 1–10,000 mGy. $^6LiF/CaF_2$:Eu also showed OSL with emission due to the 5d–4f transitions of Eu^{2+} with a peak at 430 nm during stimulation at 630 nm. A linear dose response function was confirmed over 100–10,000 mGy, and $^6LiF/CaF_2$:0.005%Eu showed the highest sensitivity.

Acknowledgements This work was supported by Grant-in-Aid for Scientific Research (A) (17H01375), Grant-in-Aid for Young Scientists (B) (17K14911) and Grant-in-Aid for Research Activity Start-up

(16H06983) from the Ministry of Education, Culture, Sports, Science and Technology of the Japanese government (MEXT) as well as A-STEP from Japan Science and Technology Agency (JST). The Cooperative Research Project of Research Institute of Electronics, Shizuoka University, Mazda Foundation, Konica Minolta Science and Technology Foundation, NAIST Foundation and TEPCO Memorial Foundation are also acknowledged.

References

1. B.C. Bhatt, Radiat. Prot. Environ. **34**, 6 (2011)
2. M.R. Mayhugh, R.W. Chrisy, N.M. Johnson, J. Appl. Phys. **41**, 2968 (1970)
3. S.W.S. McKeever, Radiat. Meas. **46**, 1336 (2011)
4. Y. Miyamoto, H. Nanto, T. Kurobori, Y. Fujimoto, T. Yanagida, J. Ueda, S. Tanabe, T. Yamamoto, Radiat. Meas. **71**, 529 (2014)
5. A.J.J. Bos, Nucl. Instrum. Methods. Res. Sect. B **184**, 3 (2001)
6. P. Bilski, P. Olko, B. Burgkhardt, E. Piesch, Radiat. Meas. **24**, 439 (1995)
7. M. Budzanowski, P. Bilski, P. Olko, E. Ryba, S. Perle, M. Majewski, Radiat. Prot. Dosim. **125**(4), 251 (2007)
8. G.F. knoll, *Radiation Detection and Measurements*, 2nd edn. (Wiley, New York, 2001)
9. M. Koshimizu, T. Yanagida, Y. Fujimoto, Y. Yamazaki, K. Watanabe, A. Uritani, K. Fukuda, N. Kawaguchi, S. Kishimoto, K. Asai, Appl. Phys. Exp. **6**, 062601 (2013)
10. T. Yanagida, A. Yamaji, N. Kawaguchi, Y. Fujimoto, K. Fukuda, S. Kurosawa, A. Yamazaki, K. Watanabe, Y. Futami, Y. Yokota, A. Uritani, T. Iguchi, A. Yoshikawa, M. Nikl, Appl. Phys. Exp. **4**, 106401 (2011)
11. T. Yanagida, N. Kawaguchi, Y. Fujimoto, K. Fukuda, Y. Yokota, A. Yamazaki, K. Watanabe, J. Pejchal, A. Uritani, T. Iguchi, A. Yoshikawa, Opt. Mater. **33**, 1243 (2011)
12. T. Yanagida, A. Yoshikawa, Y. Yokota, S. Maeo, N. Kawaguchi, S. Ishizu, K. Fukuda, T. Suyama, Opt. Mater. **32**, 311 (2009)
13. T. Fujiwara, H. Takahashi, T. Yanagida, K. Kamada, K. Fukuda, N. Kawaguchi, N.L. Yamada, M. Furusawa, K. Watanabe, Y. Fujimoto, M. Uesaka, Neutron News **23**, 31 (2012)
14. P.A. Rodnyi, V.B. Mikhailik, G.B. Stryganyuk, A.S. Voloshinovskii, C.W.E. Eijk, G.F. Zimmerer, J. Lumin. **86**, 161 (2000)
15. G. Rooh, H.J. Kim, S. Kim, IEEE Trans. Nucl. Sci. **57**, 1255 (2010)
16. G. Rooh, H.J. Kim, H. Park, S. Kim, IEEE Trans. Nucl. Sci. **57**, 3836 (2010)
17. M. Danilkin, A. Lust, M. Kerikmäe, V. Seeman, H. Mändar, M. Must, Radiat. Meas. **41**, 677 (2006)
18. V.E. Kafadar, A.N. Yazici, R.G. Yildirim, Nucl. Instrum. Methods Res. Sect. B **267**, 3337 (2009)
19. A. Choujyakh, F. Gimcno, J.I. Pena, L. Contreras, V.M. Orera, Phys. Chem. News **13**, 139 (2003)
20. J. Trohan-Piegza, J. Glodo, V.K. Sarin, Radiat. Meas. **45**, 163 (2000)
21. N. Kawaguchi, K. Fukuda, T. Yanagida, Y. Fujimoto, Y. Yokota, T. Suyama, K. Watanabe, A. Yamazaki, A. Yoshikawa, Nucl. Instrum. Methods Res. Sect. A **652**, 209 (2011)
22. T. Yanagida, N. Kawaguchi, Y. Fujimoto, K. Fukuda, K. Watanabe, A. Yamazaki, A. Uritani, J. Lumin. **144**, 212 (2013)
23. T. Yanagida, K. Fukuda, Y. Fujimoto, N. Kawaguchi, S. Kurosawa, A. Yamazaki, K. Watanabe, Y. Futami, Y. Yokota, J. Pejchal, A. Yoshikawa, A. Uritani, T. Iguchi, Opt. Mater. **34**, 209 (2012)
24. S. Kumar, A.K. Sharma, S.P. Lochab, R. Kumar, AIP Conf. Proc. **1447**, 387 (2012)
25. M. Bidyasagar, A.G. Bauna, Th..B. Singh, J. Pure. Appl. Phys. **52**, 609 (2014)
26. H. Msai, T. Yanagida, T. Mizoguchi, T. Ina, T. Miyazaki, N. Kawaguti, K. Fukuda, Sci. Rep. **5**, 13332 (2015)
27. T. Yanagida, K. Kamada, Y. Fujimoto, H. Yagi, T. Yanagitani, Opt. Mater. **35**, 2480 (2013)
28. T. Yanagida, Y. Fujimoto, T. Ito, K. Uchiyama, K. Mori, Appl. Phys. Exp. **7**, 062401 (2014)
29. T. Yanagida, Y. Fujimoto, N. Kawaguchi, S. Yanagida, J. Ceram. Soc. Jpn. **121**, 988 (2013)
30. F. Nakamura, T. Kato, G. Okada, N. Kawaguchi, K. Fukuda, T. Yanagida, Ceram. Int. **43**, 604 (2017)
31. P. Belli, R. Bernabei, V. Landoni, I. Modena, Nucl. Instrum. Methods Res. Sect. A **357**, 329 (1995)
32. Y. Nakamura, Y. Koizumi, J. Chromatogr. **333**, 83 (1985)
33. V.A. Skuratov, S.M. Abu, V.A. AlAzm, Altynov, Nucl. Instrum. Methods Res. Sect. B **191**, 251 (2002)
34. N. Fedorov, A. Belsky, E. Constant, D. Descamps, P. Martin, A.N. Vasil'ev, J. Lumin. **129**, 1813 (2009)
35. G. Kitis, J.M. Gomes-Ros, J.W.N. Tuyn, J. Phys. D **31**, 2636 (1998)